

Submillimeter Galaxies as Tracers of Mass Assembly at Large M

R. Genzel^{1,2}, A. J. Baker¹, R. J. Ivison³, F. Bertoldi⁴, A. W. Blain⁵, S. C. Chapman⁵, P. Cox⁶, R. I. Davies¹, F. Eisenhauer¹, D. T. Frayer⁷, T. Greve⁸, M. D. Lehnert¹, D. Lutz¹, N. Nesvadba¹, R. Neri⁹, A. Omont¹⁰, S. Seitz¹¹, I. Smail¹², L. J. Tacconi¹, M. Tecza¹, N. A. Thatte¹³, and R. Bender^{1,11}

¹ Max-Planck-Institut für extraterrestrische Physik (MPE), Garching, Germany

² Department of Physics, University of California, Berkeley, CA, USA

³ Astronomy Technology Centre, Royal Observatory, Edinburgh, UK

⁴ Max-Planck-Institut für Radioastronomie (MPIfR), Bonn, Germany

⁵ California Institute of Technology, Pasadena, USA

⁶ Institut d'Astrophysique Spatiale, Université de Paris Sud, Orsay, France

⁷ Spitzer Science Center, California Institute of Technology, Pasadena, USA

⁸ Institute for Astronomy, University of Edinburgh, Edinburgh, UK

⁹ Institut de Radio Astronomie Millimétrique (IRAM), Grenoble, France

¹⁰ CNRS & Université de Paris, Paris, France

¹¹ Munich University Observatory (USM), München, Germany

¹² Institute for Computational Cosmology, University of Durham, Durham, UK

¹³ University of Oxford Astrophysics, Oxford, UK

1 Introduction

Deep imaging in the rest-frame UV has constrained both the evolution of the cosmic star formation rate density [1] and its time integral, the growth of the cosmic stellar mass density [2]. Short-wavelength studies give an incomplete picture, however, since an important population of high-redshift galaxies is heavily dust-obscured. The strength of the extragalactic mid- and far-IR/submillimeter background indicates that about half of the cosmic energy density comes from dusty luminous and ultra-luminous infrared galaxies (LIRGs/ULIRGs: $L_{\text{IR}} \sim 10^{11.5}$ to $10^{13.5} L_{\odot}$) at $z \geq 1$ [3,4]. Because the brightest of these submillimeter galaxies (SMGs; see [5] and references therein) tend to lack strong X-ray emission [6], their large IR luminosities probably correspond to high star formation rates [7]. As the strikingly different appearances of the Hubble Deep Field at $0.83 \mu\text{m}$ [8] and $850 \mu\text{m}$ [9] exemplify, SMGs are rarer and forming stars much more intensely than typical optically selected systems [8,9]. Here we discuss new observations that shed light on the importance of SMGs in the history of galaxy mass assembly (all numbers assuming a flat $\Omega_A = 0.7$ cosmology with $H_0 = 70 \text{ km s}^{-1} \text{ Mpc}^{-1}$).

2 Observations: PdBI millimeter interferometry

Since SMGs in most cases have relatively poorly known positions and frequently have only weak counterparts in the rest-frame UV and optical, redshifts and

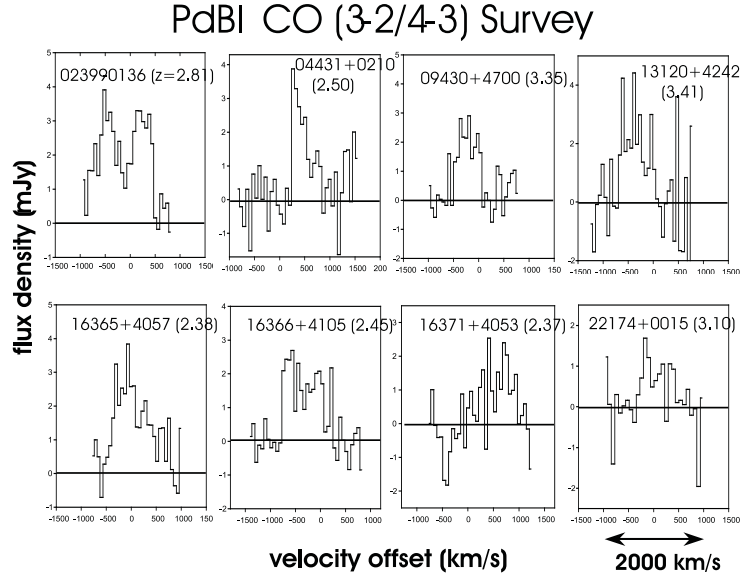


Fig. 1. Integrated CO spectra of the seven detected PdBI survey sources [11,12] plus SMMJ 02399-0136 [13]. Source names and redshifts are listed in the insets; flux density and velocity scales are the same for all sources.

spectroscopic parameters were initially confirmed with CO interferometry for only two of the few hundred detected sources [5]. Recently, a subset of the authors have initiated a new program to obtain spectroscopic redshifts with the Keck telescope for a number of sources detected with SCUBA at $850\ \mu\text{m}$, in most cases aided by more precise positions derived from deep 1.4 GHz VLA maps [10]. Here we report the first results of the millimeter follow-up of these SMGs, undertaken with the IRAM Plateau de Bure Interferometer (PdBI). In the B, C, and D configurations of the PdBI, we searched for the CO(3–2) and CO(4–3) rotational transitions (redshifted to the 3 mm atmospheric window) in a sample of so far twelve SMGs with $S_{850} \geq 5\ \text{mJy}$ and reliable UV/optical spectroscopic redshifts. Integration times per source ranged from 13 to 30 hours, for a total integration time of about 1Ms in the 2002/2003 observing season. We have detected significant CO emission in 7 out of the 12 sources, thus roughly quadrupling the number of CO-confirmed SMG redshifts [11,12]. Figure 1 shows the integrated CO(3–2/4–3) spectra for the seven new sources and for the $z = 2.81$ system SMMJ02399-0136 [13]. Figure 2 shows the integrated CO maps superposed on rest-frame UV (*I*-band) and optical (*K*-band) images of three of the sources [11].

Our PdBI observations confirm the median $z \sim 2.4$ determined from rest-frame UV/optical spectroscopy [10], although in several cases, the UV redshift is inferred from a source that is physically distinct from the SMG (e.g.,

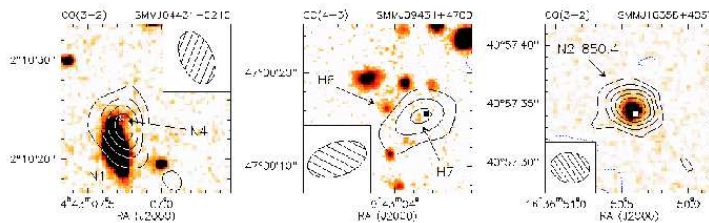


Fig. 2. Integrated CO maps of three SMGs studied with the PdBI [11], superposed on greyscale images of rest-frame UV (center panel) and optical (left and right panels) emission. FWHM synthesized beams are shown as hatched ellipses. In the left panel, the asterisk marks the position of the ERO N4 (uncertainty $\pm 0.5''$ – see text), while the edge-on spiral galaxy N1 ($2''$ SE of the CO source) lies in the foreground cluster at $z = 0.18$. In the center and right panels, filled squares mark millimeter continuum positions. Arrows show the positions of radio sources H6 and H7; the stronger of these (H6) is a narrow-line Seyfert galaxy with Ly α indicating $z = 3.349$. CO(4–3) emission from N2 850.4 remains largely unresolved.

SMM J09431+4700 in Fig. 2). SMGs likely sample very dense environments that may harbor additional, UV-bright star-forming galaxies.

SMGs are rich in molecular gas. Correcting for foreground lensing wherever appropriate (and known), and using the $M_{\text{gas}}/L_{\text{CO}}$ conversion factor appropriate for $z \sim 0.1$ ULIRGs, the median gas mass of the eight SMGs in Fig. 1 (plus the $z = 2.56$ galaxy SMM J14011+0252 [14,15]) is $2.2 \times 10^{10} M_{\odot}$. This value is similar to the median molecular gas mass found in high- z QSOs and about three times greater than in local ULIRGs. The inferred median far-IR luminosity of the sample (again corrected for lensing) is about $1.3 \times 10^{13} L_{\odot}$, corresponding to a star formation rate of about $1100 M_{\odot} \text{yr}^{-1}$.

Our most important finding is that the brightest SMGs ($S_{850} \geq 5$ mJy), contributing about 25% of the submillimeter background, have large dynamical masses. The median velocity dispersion of our sample is $255(\pm 38) \text{ km s}^{-1}$. The ratio of the squares of the median velocity dispersions then implies that our SMGs have dynamical masses at least $13(\pm 4)$ times greater than the $z \sim 3$ Lyman break galaxy (LBG) population [16], and at least $5(\pm 1.5)$ times greater than optically selected populations at $z \sim 2$ ([17] – see also this volume). There are indications that SMGs are larger than LBGs in which case these estimates are lower limits [13,11,18]. Assuming a rotating disk geometry at an inclination of 40° , the median velocity dispersion corresponds to a dynamical mass of $1.1 \times 10^{11} M_{\odot}$ within $R = 4$ kpc. Based on its spatially resolved rotation curve, SMM J02399-0136 has a total dynamical mass of $3 \times 10^{11} M_{\odot}$ within $R = 8$ kpc, half of which is probably stellar [13]. Near-IR photometry indicates that the median stellar mass for the $z \sim 3$ LBG population is $1.1 \times 10^{10} M_{\odot}$ [19], consistent

with the dynamical mass ratio estimated above. Dynamical and stellar masses of the SMGs in our sample are thus comparable to those of local m^* galaxies.

3 Observations: SPIFFI NIR integral field spectroscopy

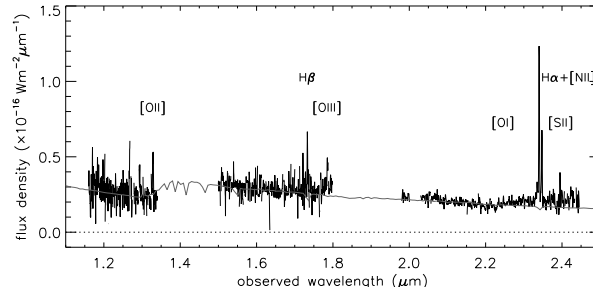


Fig. 3. J , H , and K spectra of J14011 extracted from a $2'' \times 1.5''$ aperture [22]. Superposed is the model STARS spectrum for a 200 Myr old continuous star formation episode with solar metallicity, a $1 - 100 M_{\odot}$ Salpeter IMF, and extinction $A_V = 0.7$.

We have also conducted a detailed rest-frame optical case study of the bright source SMM J14011+0252 (hereafter J14011), a $z = 2.565$ SMG lying behind the $z = 0.25$ cluster A1835 [20]. For this study we used SPIFFI, the SPectrometer for Infrared Faint Field Imaging [21], at the ESO VLT. In three runs between February and April 2003, we observed J14011 in the J , H , and K bands, with a FWHM spatial resolution of about $0.6''$ and spectral resolutions ranging from 125 to 200 km s^{-1} . SPIFFI obtains simultaneous spectra for each of 32×32 contiguous $0.25''$ pixels. The total on-source integration times were 60 minutes in J , 95 minutes in H , and 340 minutes in K [22].

Within the bright eastern J1 component of J14011, the SPIFFI data reveal substantial spatial variation in $H\alpha$ equivalent width: nebular line emission is extended over about $1''$ (lensing corrected) and is strongest away from the central continuum peak. The integrated spectrum of J1 (Fig. 3) appears to exhibit a continuum break between the observed J and H bands. The feature's most likely origin is the Balmer break of a ≥ 100 Myr old stellar population at $z \simeq 2.565$. The J1 line fluxes allow us to measure the R_{23} estimator for its oxygen abundance. After correcting for the $E(B - V) = 0.18$ implied by the Balmer decrement, we derive an oxygen abundance of 8.96 ± 0.10 , or 1.9 times solar. The observed high $[\text{NII}]/H\alpha$ ratio implies that J14011 cannot fall on the lower-metallicity branch of the $[\text{O}/\text{H}]$ vs. R_{23} relation. In contrast to the high abundances claimed for some high- z QSOs, this metallicity refers to the entire galaxy on $\sim 10 \text{ kpc}$ scales.

For a closed-box model with solar yield, this metallicity corresponds to a gas/baryonic mass fraction of $\exp(-Z/Z_{\odot}) \simeq 0.16$. From its intrinsic (corrected

for a lensing magnification of 5) gas mass of $\simeq 1.3 \times 10^{10} M_\odot$, we therefore infer a total baryonic mass $\simeq 8 \times 10^{10} M_\odot$ and stellar mass $\simeq 7 \times 10^{10} M_\odot$. This last value is empirically supported by the location of J14011 in the local mass-metallicity relation. Adopting a recent version of that relation [23], we would expect a stellar mass of $\sim 6 \times 10^{10} M_\odot$. From the closed-box model with continuous star formation at the current rate ($380 M_\odot \text{ yr}^{-1}$) we infer the overall duration of the star forming activity in J14011 to be $t_{\text{SF}} \simeq 220 \text{ Myr}$. This age is entirely consistent with the strength of the Balmer break seen in Fig. 3. As a further consistency check, we can estimate a dynamical mass for J14011 from the $\sim 2.2''$ and $\sim 180 \text{ km s}^{-1}$ separations between J1 and [second component] J2, assuming these orbit around a common center. For a predominantly north-south lensing shear, the result is $\sim 3.4 \times 10^{10} \sin^{-2} i M_\odot$, consistent with the moderately low inclination also implied by the $\text{H}\alpha$ morphology.

4 SMGs and mass assembly

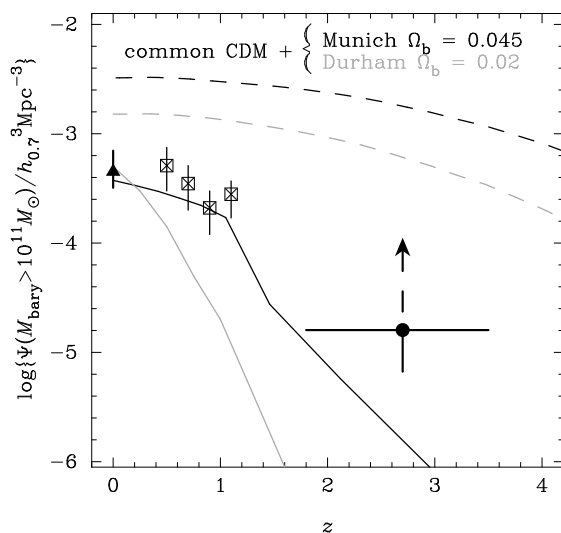


Fig. 4. Comoving number densities of galaxies with baryonic masses $\geq 10^{11} M_\odot$ as a function of redshift [22]. Triangle and open squares show densities of massive stellar systems at $z = 0$ [25] and $z \sim 1$ [26]; circle shows density for massive SMGs at $z \sim 2.7$, with a factor of 7 correction for burst lifetime. Solid curves show the predictions of semi-analytic modelling by the “Munich” and “Durham” groups [27,28]; dashed curves show the corresponding number densities of halos with *available* baryonic masses $\geq 10^{11} M_\odot$. The two models use the same halo simulations but assume different Ω_b .

Our IRAM and VLT results on metallicity and gas/dynamical mass build a compelling case that the most luminous SMGs ($S_{850} \sim 5$ to 10 mJy) have

dynamical and – within the factor 2 uncertainties of the present estimates – also stellar masses of $\sim 10^{11} M_{\odot}$. This stellar component has plausibly formed in the current starburst of duration ~ 100 Myr. How does the inferred comoving volume density of SMGs compare to theoretical models of galaxy formation?

From the observed surface density of SMGs with $S_{850} > 5$ mJy [24], we infer that radio-detected SMGs with baryonic masses $\geq 10^{11} M_{\odot}$ in the range $1.8 \leq z \leq 3.5$ have a comoving number density of $1.6_{-0.6}^{+1.0} \times 10^{-5} \text{Mpc}^{-3}$ [22]. This density needs to be corrected upward to account for sources that are in the same mass bin but no longer luminous enough to have been detected at $850 \mu\text{m}$. Relative to the 1.8 Gyr elapsed over the range $1.8 \leq z \leq 3.5$, the ~ 220 Myr age and ~ 30 Myr gas exhaustion timescale for the starburst in J14011 imply a lifetime correction factor of about 7. Figure 4 plots this prediction, together with the comoving number densities of galaxies with stellar masses above the $10^{11} M_{\odot}$ threshold at $z \sim 0$ [25] and $z \sim 1$ [26]. Also plotted are the predictions of two semi-analytic models [27,28]. Since all theoretical and observational values assume the same cosmology and a consistent (either Miller-Scalo or $1 - 100 M_{\odot}$ Salpeter) IMF, we are secure in concluding that the models underpredict the number densities of massive galaxies at $z \sim 2.5$ [22]. Couching Fig. 4 in terms of *mass* emphasizes that the observed surface densities of SMGs cannot be explained using a very flat IMF alone. We also note that the models contain enough dark halos of total mass $\geq 10^{11} (\Omega_{\text{M}}/\Omega_{\text{b}}) M_{\odot}$ to account for the observed comoving number densities of massive SMGs, provided all of their baryons can be rapidly and efficiently assembled into galaxies. SMGs thus impose a powerful “baryonic mass assembly” test at the upper end of the galaxy mass function [13].

Our correction of the observed number density of SMGs to account for their less dust-luminous descendants raises the question of what types of galaxies SMGs can plausibly evolve into. Although LBGs are clearly excluded due to their smaller masses, an intriguing alternative is the newly identified population whose red $J - K$ colors can stem from a strong Balmer break at $z \sim 2.5$ [29]. These galaxies appear to be strongly clustered [30] and – assuming a uniform distribution in the redshift range $2 \leq z \leq 3.5$ [31] – have a comoving number density $\sim 1.8 \times 10^{-4} \text{Mpc}^{-3}$. Relatively few sources with red $J - K$ colors are also luminous (sub)millimeter emitters, indicating that the two populations have little direct overlap. With three examples in the HDF-S having (for a Miller-Scalo IMF) stellar masses $(0.6 - 1.4) \times 10^{11} M_{\odot}$ [32], it would seem plausible that the more luminous objects with red $J - K$ colors at this epoch could have passed through a SMG phase at higher redshift.

References

1. P. Madau, H. C. Ferguson, M. E. Dickinson, et al.: MNRAS, **283**, 1388 (1996)
2. M. Dickinson, C. Papovich, H. C. Ferguson, T. Budavári: ApJ, **587**, 25 (2003)
3. J.-L. Puget, A. Abergel, J. P. Bernard, F. Boulanger, et al.: A&A, **308**, L5 (1996)
4. Y. C. Pei, M. S. Fall, M. G. Hauser: ApJ, **522**, 604 (1999)
5. A. W. Blain, I. Smail, R. J. Ivison, et al.: Physics Reports, **369**, 111 (2002)

6. O. Almaini, S. E. Scott, J. S. Dunlop, et al.: MNRAS, **338**, 303 (2003)
7. A. J. Barger, L. L. Cowie, E. A. Richards: AJ, **119**, 2092 (2000)
8. R. E. Williams, B. Blacker, M. Dickinson, et al.: AJ, **112**, 1335 (1996)
9. D. H. Hughes, S. Serjeant, J. Dunlop, et al.: Nature, **394**, 241 (1998)
10. S. C. Chapman, A. W. Blain, R. J. Ivison, I. Smail: Nature, **422**, 695 (2003)
11. R. Neri, R. Genzel, R. J. Ivison, F. Bertoldi, et al.: ApJ, **597**, L113 (2003)
12. T. Greve, et al.: in preparation (2004)
13. R. Genzel, A. J. Baker, L. J. Tacconi, D. Lutz, P. Cox, et al.: ApJ, **584**, 633 (2003)
14. D. T. Frayer, R. J. Ivison, N. Z. Scoville, A. S. Evans, et al.: ApJ, **514**, L13 (1999)
15. D. Downes, P. M. Solomon: ApJ, **582**, 37 (2003)
16. M. Pettini, A. E. Shapley, C. C. Steidel, J.-G. Cuby, et al.: ApJ, **554**, 981 (2001)
17. D. K. Erb, A. E. Shapley, C. C. Steidel, M. Pettini, et al.: ApJ, **591**, 101 (2003)
18. S. C. Chapman, et al.: in preparation (2004)
19. A. E. Shapley, C. C. Steidel, K. L. Adelberger, et al.: ApJ, **562**, 95 (2001)
20. R. J. Ivison, I. Smail, D. T. Frayer, J.-P. Kneib, A. W. Blain: ApJ, **561**, L45 (2001)
21. F. Eisenhauer, M. Tecza, N. A. Thatte, et al.: The ESO Messenger, **113**, 17 (2003)
22. M. Tecza, A. J. Baker, R. I. Davies, R. Genzel, et al.: ApJL, submitted (2004)
23. C. A. Tremonti, T. M. Heckman, G. Kauffmann, et al.: ApJ, submitted (2004)
24. I. Smail, R. J. Ivison, A. W. Blain, J.-P. Kneib: MNRAS, **331**, 495 (2002)
25. S. Cole, P. Norberg, C. M. Baugh, C. S. Frenk, et al.: MNRAS, **326**, 255, (2001)
26. N. Drory, R. Bender, J. Snigula, G. Feulner, U. Hopp, C. Maraston, et al.: ‘The Mass Function of Field Galaxies at $0.4 < z < 1.2$ as Derived From the MUNICS K -Selected Sample’, in *The Masses of Galaxies at Low and High Redshift*, ed. by R. Bender, A. Renzini (Berlin, Springer Verlag, 2003), pp. 140–145
27. G. Kauffmann, J. M. Colberg, et al.: MNRAS, **303**, 188 (1999)
28. C. M. Baugh, A. J. Benson, S. Cole, C. S. Frenk, C. Lacey: ‘The Evolution of Galaxy Mass in Hierarchical Models’, in *The Masses of Galaxies at Low and High Redshift*, ed. by R. Bender, A. Renzini (Berlin, Springer Verlag, 2003), pp. 91–96
29. M. Franx, I. Labbé, G. Rudnick, P. G. van Dokkum, et al.: ApJ, **587**, L79 (2003)
30. E. Daddi, H. J. A. Röttgering, I. Labbé, G. Rudnick, et al.: ApJ, **588**, 50 (2003)
31. P. G. van Dokkum, N. M. Förster Schreiber, M. Franx, et al.: ApJ, **587**, L83 (2003)
32. P. Saracco, M. Longhetti, et al.: A&A, submitted (2004, astro-ph/0310131)